# Impact of noncoplanar degrees of freedom on quasifission contributions with the estimation of unobserved decay channels for the study of $^{196}$Pt* using the dynamical cluster-decay model

Sahila Chopra,[1] Manoj K. Sharma,[2] Peter Oto Hess,[3,4] Hemdeep,[1] and NeetuMaan[1]
[1]*Department of Physics, Panjab University, Chandigarh 160014, India*
[2]*School of Physics and Material Science, Thapar University, Patiala 147004, India*
[3]*Instituto de Ciencias Nucleares, UNAM, 04510 Mexico City, Mexico*
[4]*Frankfurt Institute for Advanced Studies, J. W. von Goethe University, Frankfurt, Germany*

(Received 1 March 2021; accepted 10 June 2021; published 25 June 2021)

In Phys. Rev. C **98**, 041603 (2018) it was demonstrated that the noncoplanar degrees of freedom (or azimuthal angle $\Phi_c \neq 0^0$), including higher-multipole deformations $\beta_{\lambda i}$ ($\lambda = 2, 3, 4;\ i = 1, 2$), and the compact orientations $\theta_{ci}$ are the most essential set of parameters in the dynamical cluster-decay model (DCM), in order to study heavy-ion reactions. In this work, we study the comparison between the coplanar ($\Phi = 0^\circ$) and noncoplanar ($\Phi_c \neq 0^\circ$) configurations, including higher multipole deformations, for $^{196}$Pt* formed via the $^{132}$Sn + $^{64}$Ni reaction. This reaction was earlier studied [M. K. Sharma *et al.*, J. Phys. G: Nucl. Part. Phys. **38**, 055104 (2011)] by one of our collaborators but only with $\Phi = 0^\circ$, including quadrupole deformations, $\beta_{2i}$ alone having "optimum" orientations ($\theta_{\text{opt.}}$), with the result of noncompound nucleus [nCN, equivalently quasi-fission (qf)] contribution at higher energies. The only parameter of the DCM is the neck length $\Delta R$, whose value for the nuclear proximity potential used here remains within its range of validity (≈2 fm). The evaporation residues (ERs) and fission cross section ($\sigma_{ff}$) are calculated in reference to available experimental data at near- and sub-barrier energies for $^{196}$Pt*. As a result of inclusion of $\Phi_c \neq 0^\circ$, the nCN contribution approaches zero at higher energies and corresponds to $P_{\text{CN}} = 1$, which is rather significant for the $\Phi = 0^\circ$ configuration. Secondly, in this attempt we have tried to explore the evolution of the neck-length parameter ($\Delta R$), which will help us to estimate the cross sections of unobserved decay channels.

DOI: 10.1103/PhysRevC.103.064615

## I. INTRODUCTION

The main focus of this work is to study the effect of noncoplanar degrees of freedom along with the higher-multipole deformations $\beta_{\lambda i}$ ($\lambda = 2, 3, 4;\ i = 1, 2$), and compact orientations $\theta_{ci}$ in the study of heavy-ion reactions. Next, we would like to scrutinize the capability of the neck-length parameter ($\Delta R$ or reaction time) to estimate (or predict) the cross sections of unobserved decay channels using the dynamical cluster-decay model (DCM) of Gupta and collaborators (see, e.g., the reviews [1,2]). We use the available experimental data of $^{196}$Pt* formed via $^{132}$Sn + $^{64}$Ni, where the experimental data for evaporation residues ($\sigma_{\text{ER}}$) and fission cross sections ($\sigma_{ff}$) [3] are at different center-of-mass energies ($E_{\text{c.m.}}$). The experimental data are available at eleven center-of-mass energies for the evaporation residues, while the fission channel is explored at only five energies. To analyze the capability of $\Delta R$ to estimate the cross section for unobserved decay channels, we have taken $E_{\text{c.m.}} = 167.2$ MeV, where only $\sigma_{\text{ER}}$ has been measured and in this work our calculations correspond to the estimated cross section $\sigma_{ff}$. We have taken only one energy ($E_{\text{c.m.}} = 167.2$ MeV) to explore the strength of $\Delta R$ to predict (more correctly estimate) the cross sections of unobserved decay channels, because only this energy is missing from the group of five energies [$E_{\text{c.m.}} = 195.2$, 183.7, 175.2, 171, **(167.2)**, 165.5 MeV] where $\sigma_{ff}$ is not given experimentally. So, this energy could give more strength to the predictability of $\Delta R$ in the case of unobserved decay channels after following the same trend as at the other energies.

In the previous study of $^{196}$Pt* [4] within the DCM, for the set of parameters [coplanar degrees of freedom, $\Phi = 0^\circ$, quadrupole deformations ($\beta_{2i}$ alone), and "optimum" orientations ($\theta_{\text{opt.}}$)], the noncompound nucleus [nCN, equivalently quasifission (qf)] contribution for the $\sigma_{ff}$ at higher two energies is very high with best fitted $\sigma_{\text{ER}}$ at all energies. So, first we would like to study the nCN cross section ($\sigma_{nCN}$) at higher energies, where $\sigma_{ff}$ shows significant nCN contribution. We have two purposes to study $^{196}$Pt* using $\Phi_c \neq 0^\circ$: (i) to check the impact of $\Phi_c \neq 0^\circ$ on nCN contribution and (ii) to explore the possibility for existence of un-observed decay channels in the reaction dynamics. We have aimed to exercise the predictability of decay cross sections of unobserved channels.

Interestingly, $^{196}$Pt* is a pure CN (nCN = 0) at all energies, for noncoplanar degrees of freedom ($\Phi_c \neq 0^\circ$), including higher-multipole deformations $\beta_{\lambda i}$ ($\lambda = 2, 3, 4;\ i = 1, 2$) and compact orientations $\theta_{ci}$. However, there is a significant noncompound nucleus contribution (nCN $\neq 0$) at higher two energies for $\Phi = 0^\circ$ (coplanar) along with two different set of parameters, given as (i) quadrupole deformations ($\beta_{2i}$ alone), $\theta_{\text{opt.}}$; (ii) higher-multipole deformations including up to hexadecupole deformations ($\beta_2$–$\beta_4$) and compact orientations $\theta_{ci}$.

 

Note that the above calculations refer to the in-built property of the DCM, i.e., "barrier modification" related to the reaction timescale ($\Delta R$), which will be most of the time lower in the case of $\Phi_c \neq 0^\circ$ than in $\Phi = 0^\circ$, i.e., the parameter $\Delta R$ for the nCN contribution is smaller and hence the reaction time larger than for the CN decay process. We have also agreed with the general aspect of the presence of the quasifission contribution at higher energies but experimentally $^{196}$Pt$^*$ is a pure compound nucleus at all energies. However, we are taking experimental cross sections as reference because these data have been reproduced via coupled-channel calculations by including nuclear deformation and inelastic excitation, which makes the experimental data trustworthy. Secondly, the main interest here is to highlight the relevance of noncoplanar degrees of freedom along with the higher-multipole deformations. The higher-multipole deformations $\beta_{\lambda i}$ ($\lambda = 2, 3, 4;\ i = 1, 2$) together with noncoplanar $\Phi_c \neq 0^\circ$ configuration provide important additional degrees of freedom for approximate address of a compound nucleus fusion reaction. We have studied [5] very significant results using the noncoplanar degree of freedom ($\Phi = 0^\circ$), in the case of heavy-ion reactions (HIR) at low energy within the framework of the dynamical cluster-decay model. There are a few reasons to take this configuration as a significant one; e.g., in the case of $^{105}$Ag$^*$ formed in the $^{12}$C + $^{93}$Nb reaction at below barrier energies for the $\Phi = 0^\circ$ case, $P_{\rm CN}$ and $P_{\rm surv}$ show different variations with respect to $E_{\rm c.m.}$, but for $\Phi_c \neq 0^\circ$ both $P_{\rm CN}$ and $P_{\rm surv}$ of $^{105}$Ag$^*$ are decreasing functions of $E_{\rm c.m.}$, and hence belong to the category of weakly fissioning nuclei, whereas for the case of $\Phi = 0^\circ$ the $P_{\rm CN}$ is an increasing function of $E_{\rm c.m.}$, as in strongly fissioning superheavy nuclei. In the case of CN $^{220}$Th$^*$, we have found that the outcome remain the same in both the cases $\Phi = 0^\circ$ and $\Phi_c \neq 0^\circ$: the $3n$ and $5n$ decays are always pure CN decays and the $4n$ decay is mainly of nCN content.

In our recent published work [5], we showed that $\Phi_c \neq 0^\circ$ (with $\beta_2$–$\beta_4$, $\theta_{ci}$) is a compound-nucleus-specific degree of freedom. The result will not diverge from the real output of a nuclear reaction; in fact it is the most probable configuration to study the compound nucleus decay process. We have noticed a large amount of nCN contribution from the previously studied cases of Pt isotopes; i.e., in the case of $^{196}$Pt$^*$, with $\beta_{2i}$ alone and "optimum" configuration ($\Phi = 0^\circ$), at higher two energies we found 48% and 15% nCN contribution in $\sigma_{ff}$. However, $\sigma_{\rm ER}$ is perfectly fitted with the experimental data, and with deformations $\beta_2$–$\beta_4$ and compact orientations $\theta_{ci}$ the constitution of nCN component becomes negligibly small and CN-fusion probability $P_{\rm CN}$ increases once we move from $\Phi = 0^\circ$ to $\Phi_c \neq 0^\circ$.

The paper is organized as follows. Section II gives a brief description of the dynamical cluster-decay model (DCM). Our calculations for the $^{132}$Sn + $^{64}$Ni reaction, using deformed and noncoplanar oriented nuclei, are given in Sec. III. A comparison is also carried out with the case of coplanar nuclei. Finally, a summary and conclusions of our work are presented in Sec. IV. Brief contributions from this work were made at the International Conference on Nuclear Physics, March 15–18, 2017, at the Department of Physics, Panjab University, Chandigarh.

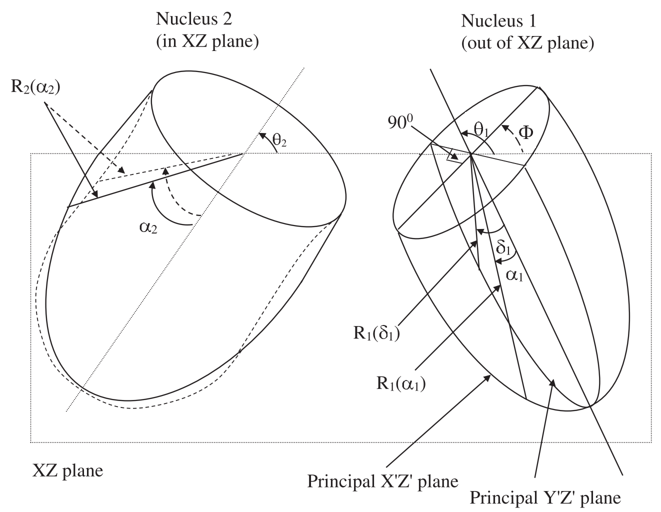


FIG. 1. Two unequal nuclei (here one $\beta_2$ deformed and the other up to $\beta_4$), oriented at angles $\theta_1$ and $\theta_2$, with their principal planes $X'Z'$ and $XZ$ forming an azimuthal angle $\Phi$. The angle $\Phi$ is shown by a dashed line, since it is meant to be an angle coming out of plane $XZ$. Nucleus 2 is in the $XZ$ plane and for the out-of-plane nucleus 1 another principal plane $Y'Z'$, perpendicular to $X'Z'$, is also shown. Only lower halves of the two nuclei are shown. This figure is based on Fig. 1 of Ref. [6].

## II. THE DYNAMICAL CLUSTER-DECAY MODEL (DCM)

The dynamical cluster-decay model (DCM) assumes that the compound nucleus is formed (in the entrance channel) with transmission probability $T_\ell$. Its decay is studied in terms of collective coordinates of mass (and charge) asymmetries $\eta$ (and $\eta_Z$) [$\eta = (A_1 - A_2)/(A_1 + A_2)$ [7], $\eta_Z = (Z_1 - Z_2)/(Z_1 + Z_2)$ [8]] and relative separation $R$, with multipole deformations $\beta_{\lambda i}$ ($\lambda = 2, 3, 4;\ i = 1, 2$), orientations $\theta_i$, and the azimuthal angle $\Phi$ between the principle planes of two nuclei (see Fig. 1, where only lower halves of the two nuclei are shown; for other details, see also Refs. [5,6]). In DCM, the dynamical fragmentation theory characterizes (i) the nucleon division (or exchange) between outgoing fragments and (ii) the transfer of kinetic energy of the incident channel to internal excitation (total excitation or total kinetic energy (TXE or TKE) of the outgoing channel, at which the process is calculated, depending also on temperature $T$. This energy transfer process follows the relation

$$E^*_{\rm CN} + Q_{\rm out}(T) = E_{\rm c.m.} + Q_{\rm in} = {\rm TKE}(T) + {\rm TXE}(T). \quad (1)$$

The CN excitation energy $E^*_{\rm CN}$ is related to temperature $T$ (in MeV) via the relation

$$E^* = E_{\rm c.m.} + Q_{\rm in} = \frac{1}{a}AT^2 - T \quad (T \text{ in MeV}), \quad (2)$$

with level density parameter, $a = 9$ or 10, respectively, for intermediate mass or superheavy systems. In this case we have taken $a = 9$ and $Q_{\rm in}$ is the entrance channel $Q$ value.

The DCM defines the CN decay cross section in terms of $\ell$ partial waves, for each pair of fragments $(A_1, A_2)$, as

$$\sigma_{(A_1,A_2)} = \frac{\pi}{k^2}\sum_{\ell=0}^{\ell_{\max}}(2\ell+1)P_0PT_\ell, \quad k = \sqrt{\frac{2\mu E_{\rm c.m.}}{\hbar^2}}, \quad (3)$$

with $T_\ell = 1$ for $\ell \leqslant \ell_{\max}$, and zero otherwise. Here, the relative preformation probability $P_0$ refers to $\eta$ motion and $P$, the penetration probability, refers to the $R$ motion. $P$ and $P_0$ both are dependent on angular momentum $\ell$ and temperature $T$.

The formula (3), with $T_\ell = 1$, is also applicable to $\sigma_{nCN}$, which is calculated as the qf decay channel where $P_0 = 1$. Since for qf the fragments are considered not to lose their identity, the $P$ is calculated only for the incoming channel $\eta_{ic}$:

$$\sigma_{nCN} = \frac{\pi}{k^2}\sum_{\ell=0}^{\ell_{\max}}(2\ell+1)P_{\eta_{ic}}. \tag{4}$$

Note that the DCM does not account for the noncompound emission of particles, but gives only the empirically estimated nCN contribution in the CN (total) fusion cross section. Since Eq. (3) is defined in terms of the exit/decay channels alone, i.e., both the formation $P_0$ and then their emission via barrier penetration $P$ are calculated only for decay channels $(A_1, A_2)$, it follows from Eq. (1) that

$$\sigma_{\rm ER} = \sum_{A_2=1}^{4 \text{ or } 5}\sigma_{(A_1,A_2)} \quad \text{or} \quad = \sum_{x=1}^{4 \text{ or } 5}\sigma_{xn} \tag{5}$$

and

$$\sigma_{ff} = 2\sum_{A/2-x}^{A/2}\sigma_{(A_1,A_2)}, \tag{6}$$

where $\sigma_{\rm CN} = \sigma_{\rm ER} + \sigma_{ff}$. Equation (6) is applicable to the fission cross section ($\sigma_{ff}$) in the region $A/2 \pm 22$, and according to Eq. (6) we can calculate the cross section of one side $(A/2 - 22)$ and then multiply by 2 to get the cross section of the complete fission region $A/2 \pm 22$.

The nCN contribution, obtained empirically as the difference between the experimentally measured fusion cross section and our calculated pure-CN components, i.e., $\sigma_{n\rm CN}^{\rm emp.} = \sigma_{\rm fusion}^{\rm Expt.} - \sigma_{\rm CN}^{\rm Cal.}$, where the CN fusion cross-section $\sigma_{\rm CN}$ is the sum of evaporation residue (ER) cross-section $\sigma_{\rm ER}$ and fusion-fission (ff) cross section ($\sigma_{\rm CN}^{\rm Cal.} = \sigma_{\rm ER}^{\rm Cal.} + \sigma_{ff}^{\rm Cal.}$), and $\sigma_{\rm fusion}^{\rm Cal.} = \sigma_{\rm CN}^{\rm Cal.} + \sigma_{nCN}^{\rm Cal.}$, which further allow us calculate the CN fusion probability $P_{\rm CN}$, defined as

$$P_{\rm CN} = \frac{\sigma_{\rm CN}^{\rm Cal.}}{\sigma_{\rm fusion}^{\rm Cal.}} = 1 - \frac{\sigma_{nCN}^{\rm emp.}}{\sigma_{\rm fusion}^{\rm Cal.}}. \tag{7}$$

$P_0$ is the solution of the stationary Schrödinger equation in $\eta$, at a fixed $R = R_a$:

$$\left\{-\frac{\hbar^2}{2\sqrt{B_{\eta\eta}}}\frac{\partial}{\partial\eta}\frac{1}{\sqrt{B_{\eta\eta}}}\frac{\partial}{\partial\eta} + V(R,\eta,T)\right\}\psi^\nu(\eta) = E^\nu\psi^\nu(\eta), \tag{8}$$

with $\nu = 0, 1, 2, 3, \ldots$ referring to ground-state ($\nu = 0$) and excited-states solutions. Then, the probability is given by

$$P_0(A_i) = \mid \psi(\eta(A_i)) \mid^2 \sqrt{B_{\eta\eta}}\frac{2}{A}, \tag{9}$$

where, for a Boltzmann-like function,

$$|\psi|^2 = \sum_{\nu=0}^{\infty}|\psi^\nu|^2\exp(-E^\nu/T). \tag{10}$$

For the position $R = R_a$, the first turning point for calculating the penetration $P$, in the decay of a hot CN, we use the postulate [9–11]

$$\begin{aligned} R_a(T) &= R_1(\alpha_1, T) + R_2(\alpha_2, T) + \Delta R(\eta, T), \\ &= R_t(\alpha, \eta, T) + \Delta R(\eta, T), \end{aligned} \tag{11}$$

with radius vectors

$$R_i(\alpha_i, T) = R_{0i}(T)\left[1 + \sum_\lambda \beta_{\lambda i}Y_\lambda^{(0)}(\alpha_i)\right], \tag{12}$$

and temperature-dependent nuclear radii $R_{0i}(T)$ for the equivalent spherical nuclei [12],

$$R_{0i} = \left[1.28A_i^{1/3} - 0.76 + 0.8A_i^{-1/3}\right](1 + 0.0007T^2). \tag{13}$$

The only parameter of the model $\Delta R(T)$, the neck-length parameter, is $T$ dependent, defining the first turning point $R_a$ in Eq. (11). $\Delta R(\eta, T)$ assimilates the deformation and neck formation effects between two nuclei, introduced within the extended model of Gupta and collaborators [13–15]. This method of introducing a neck-length parameter $\Delta R$ is similar to that used in both the scission-point [16] and saddle-point [17,18] statistical fission models.

The choice of the parameter $R_a$ (equivalently, $\Delta R$) in Eq. (11), for a best fit to the data, allows us to relate in a simple way the $V(R_a, \ell)$ to the top of the barrier $V_B(\ell)$ for each $\ell$, by defining their difference $\Delta V_B(\ell)$ as the effective "lowering of the barrier":

$$\Delta V_B(\ell) = V(R_a, \ell) - V_B(\ell). \tag{14}$$

Note, $\Delta V_B$ for each $\ell$ is defined as a negative quantity since the actually used barrier is effectively lowered. This is illustrated in Fig. 2 for the $\ell_{\max}$ value, fixed for light-particles [here, e.g., $x$ neutrons, $xn$, $x$ = 1–(4 or 5)] cross-section $\sigma_{xn}(\ell) \to 0$ (or the penetrability starts to contribute, i.e., $P_0 > 10^{-10}$ for the example studied here; see Fig. 4). Thus, the fitting parameter $\Delta R$ controls the "barrier lowering" $\Delta V_B$.

The collective fragmentation potential $V_R(\eta, T)$ in Eq. (15), that brings in the structure effects of the CN into the formalism, is calculated according to the Strutinsky renormalization procedure ($B = V_{LDM} + \delta U$; $B$ is binding energy), as

$$\begin{aligned} V_R(\eta, T) = &-\sum_{i=1}^{2}[V_{LDM}(A_i, Z_i, T)] + \sum_{i=1}^{2}[\delta U_i]\exp\left(-\frac{T^2}{T_0^2}\right) \\ &+ V_P(R, A_i, \beta_{\lambda i}, \theta_i, \Phi, T) + V_C(R, Z_i, \beta_{\lambda i}, \theta_i, \Phi, T) \\ &+ V_\ell(R, A_i, \beta_{\lambda i}, \theta_i, \Phi, T), \end{aligned} \tag{15}$$

where $V_C$, $V_P$, and $V_\ell$ are the Coulomb, nuclear proximity and angular momentum dependent potentials for deformed, oriented (coplanar or noncoplanar) nuclei, all $T$ dependent. $\delta U$ are the "empirical" shell corrections of Myers and Swiatecki [19] for spherical nuclei, also made $T$ dependent to vanish exponentially with $T_0 = 1.5$ MeV [20], and $V_{LDM}$ is the $T$-dependent liquid drop energy of Davidson *et al.* [21] with its constants at $T = 0$ refitted by some of us [10,11,22] to give the experimental binding energies of Audi *et al.* [23]. Thus, in fact, we are using experimental binding energies, split into $V_{LDM}$ and $\delta U$ components. The mass parameters, $B_{\eta\eta}$,

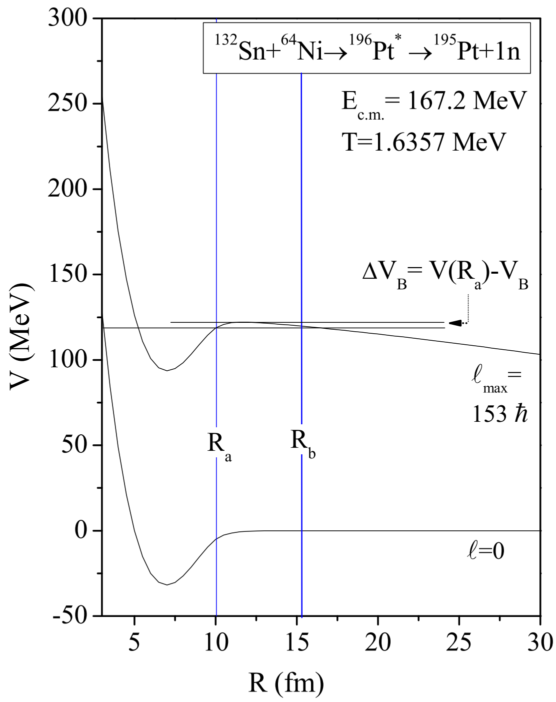


FIG. 2. The $\ell$-dependent scattering potential $V(R)$ for $^{196}$Pt $+1n$, in the decay of $^{196}$Pt$^*$ formed in the $^{132}$Sn + $^{64}$Ni reaction at $E_{\rm c.m.}$ = 167.2 MeV. The concept of barrier lowering $\Delta V_B = V(R_a) - V_B$ is also shown in this figure for the $\ell_{\rm max} = 153\hbar$ value. The first and second turning points $R_a$ and $R_b$ are also labeled.

used are the smooth classical hydrodynamical masses [24], since at large $T$ values the shell effects are almost completely washed out. For smaller $T$ (<1.5 MeV), in principle, the shell corrected masses should be used, like the cranking masses which depend on the underlying shell model basis.

To calculate the cross sections for noncoplanar nuclei ($\Phi \neq 0^\circ$), we use the same formalism as for $\Phi = 0^\circ$ (see Ref. [25]), but for the out-of-plane nucleus ($i$ = 1 or 2) we replace the corresponding radius parameter $R_i(\alpha_i)$ with its projected radius parameter $R_i^P(\alpha_i)$ in both the Coulomb and proximity potentials [6]. For the Coulomb potential radius parameter enters via $R_i(\alpha_i)$ itself and for the proximity potential via the definitions of both the mean curvature radius $\bar{R}$ and the shortest distance $s_0$, i.e., compact configurations with orientations $\theta_{ci}$ and $\Phi_c$ [26,27]. For compact configurations the interaction radius is smallest and the barrier is highest.

The $R_i^P(\alpha_i)$ is determined by defining, for the out-of-plane nucleus, two principal planes $X'Z'$ and $Y'Z'$, respectively, with radius parameters $R_i(\alpha_i)$ and $R_j(\delta_j)$, such that their projections into the plane ($XZ$) of the other nucleus are (see Fig. 1)

$$R_i^P(\alpha_i) = R_i(\alpha_i)\cos\Phi, \quad i = 1 \text{ or } 2, \tag{16}$$

and

$$R_j^P(\delta_j) = R_j(\delta_j)\cos(\Phi - \delta_j), \quad j = i = 1 \text{ or } 2. \tag{17}$$

Then, maximizing $R_j(\delta_j)$ in angle $\delta_j$, we get

$$\begin{aligned} R_i^P(\alpha_i) &= R_i^P(\alpha_i = 0^\circ) + R_i^P(\alpha_i \neq 0^\circ) \\ &= R_j^P\left(\delta_j^{\rm max}\right) + R_i(\alpha_i \neq 0^\circ)\cos\Phi, \end{aligned} \tag{18}$$

with $\delta_j^{\rm max}$ given by the condition (for fixed $\Phi$),

$$\tan(\Phi - \delta_j) = -\frac{R_j'(\delta_j)}{R_j(\delta_j)}. \tag{19}$$

Thus, the $\Phi$ dependence of the projected radius vector $R_i^P(\alpha_i)$ is also contained in maximizing $R_j^P(\delta_j^{\rm max})$. For further details, see [6]. Then, for the nuclear proximity potential—denoted by $V_P^{12}$, the potential for the nucleus 1 to be out of plane, and by $V_P^{21}$, the potential for the nucleus 2 to be out of plane—the effective nuclear proximity potential is

$$V_P = \tfrac{1}{2}\left[V_P^{12} + V_P^{21}\right]. \tag{20}$$

The penetrability $P$ in Eq. (3) or (4) is the WKB integral,

$$P = \exp\left(-\frac{2}{\hbar}\int_{R_a}^{R_b}\{2\mu[V(R,T) - Q_{\rm eff}]\}^{1/2}dR\right), \tag{21}$$

solved analytically [28,29], with the second turning point $R_b$ (see Fig. 2) satisfying

$$V(R_a) = V(R_b) = Q_{\rm eff}. \tag{22}$$

As the $\ell$ value increases, the $Q_{\rm eff}(T)$ increases and hence $V(R_a, \ell)$ also increases. Thus, $R_a$ acts like a parameter through $\Delta R(\eta, T)$ and we define that $R_a$ is the same for all $\ell$ values, i.e., $V(R_a) = Q_{\rm eff}(T, \ell = 0)$. This is required because we do not know how to add the $\ell$ effects in the binding energies.

## III. CALCULATIONS AND RESULTS

In this section, we present our calculations on the investigation the role of noncoplanar degrees of freedom $\Phi$ on calculated evaporation residues $\sigma_{\rm ER}^{\rm Cal.}$ and fission cross sections $\sigma_{\rm fission}^{\rm Cal.}$, of $^{196}$Pt$^*$ formed in the $^{132}$Sn + $^{64}$Ni reaction, at five center-of-mass energies $E_{\rm c.m.}$. As we mentioned in the Introduction, the experimentally observed decay channels for these reactions are the evaporation residues (ER) and the fission region (ff). The earlier calculations for $\Phi = 0^\circ$ (coplanar nuclei, with "optimum" configuration only) [4], showed a considerable amount of noncompound nucleus (nCN) content in the $\sigma_{\rm fission}^{\rm Cal.}$ at two higher energies and the major contribution of $A/2 \pm 22$ comes from the asymmetric fragments; however, the $\sigma_{\rm ER}^{\rm Cal.}$ was addressed at all energies. Therefore, following the prescription of Ref. [27] we first calculated the compact orientations $\theta_{ci}$ and $\Phi_c$ for all the possible fragments ($A_1, A_2$), to study the effect of noncoplanarity on the nCN contribution for $^{196}$Pt$^*$. In the following, we show that inclusion of the $\Phi$ degree of freedom modifies the result of $^{196}$Pt$^*$ ($\Phi = 0^\circ$, $\beta_2$ alone) in a significant manner, which [4] shows the contributions of nCN of almost 48% and 15% in the fission region at two higher energies.

Table I presents the DCM-calculated CN cross section $\sigma_{\rm CN}^{\rm Cal.}$ and the nCN contribution $\sigma_{nCN}^{\rm emp.}$ (calculated as $\sigma_{\rm fusion}^{\rm Expt.} - \sigma_{\rm CN}^{\rm Cal.}$) for both cases $\Phi_c = 0^\circ$ and $\Phi_c \neq 0^\circ$. Earlier calculations [4] using the $\Phi = 0^\circ$ configuration, including quadrupole deformations ($\beta_{2i}$ alone) and "optimum" orientations ($\theta_{\rm opt.}$), showed a noticeable amount of nCN at higher energies of the fission region. In this work we checked the effect of higher multipole deformations ($\beta_2 - \beta_4$) using co-planar and noncoplanar configurations and found some interesting outcomes.

TABLE I. DCM-calculated evaporation residues (ERs) and fusion-fission (ff region $= A/2 \pm 22$) cross sections for best fitted $\Delta R$'s, compared with experimental data taken from (Ref. [4]), with the included $\beta_2$–$\beta_4$ deformations for both the configurations $\Phi_c = 0^\circ$ and $\Phi_c \neq 0^\circ$.

| | $\sigma_{\mathrm{CN}}^{\mathrm{Cal.}}$ | | | | | $\sigma_{nCN}^{\mathrm{emp.}}$ | |
|---|---|---|---|---|---|---|---|
| | $\Phi_c = 0^\circ$ | | $\Phi_c \neq 0^\circ$ | | | $\Phi_c = 0^\circ$ | $\Phi_c \neq 0^\circ$ |
| Decay channel | $\Delta R$ (fm) | $\sigma_{\mathrm{ER},ff}^{\mathrm{Cal.}}$ (mb) | $\Delta R$ (fm) | $\sigma_{\mathrm{ER},ff}^{\mathrm{Cal.}}$ (mb) | $\sigma^{\mathrm{Expt.}}$ (mb) | $\sigma_{nCN}^{\mathrm{emp.}}$ (mb) | $\sigma_{nCN}^{\mathrm{emp.}}$ (mb) |
| | | | $E_{\mathrm{c.m.}} = 195.2$ MeV | | | | |
| ER | 1.6895 | 259 | 1.6556 | 258 | 259 | 0 | 0 |
| ff | 1.1599 | 392 | 1.251 | 542 | 544 | 152 | 0 |
| | | | $E_{\mathrm{c.m.}} = 183.7$ MeV | | | | |
| ER | 1.6764 | 251 | 1.6605 | 251 | 251.4 | 0 | 0 |
| ff | 1.1365 | 322 | 1.1425 | 370 | 371 | 49 | 0 |
| | | | $E_{\mathrm{c.m.}} = 175.2$ MeV | | | | |
| ER | 1.6558 | 264 | 1.6864 | 265 | 264.8 | 0 | 0 |
| ff | 1.079 | 232 | 1.0970 | 232 | 232.9 | 0 | 0 |
| | | | $E_{\mathrm{c.m.}} = 171$ MeV | | | | |
| ER | 1.6984 | 218 | 1.6513 | 218 | 218 | 0 | 0 |
| ff | 0.993 | 138.2 | 1.0483 | 138 | 138 | 0 | 0 |
| | | | $E_{\mathrm{c.m.}} = 165.5$ MeV | | | | |
| ER | 1.6922 | 184 | 1.6434 | 184 | 184 | 0 | 0 |
| ff | 0.8906 | 31.4 | 0.9077 | 31.2 | 31.2 | 0 | 0 |

For the case $\Phi_c = 0^\circ$ there was significant disagreement among the calculated and experimental fission cross sections, which on the other hand improved remarkably after using the $\Phi_c \neq 0^\circ$ configuration. It means the configuration of noncoplanar degrees of freedom along with the higher multipole deformations provides a better set of parameters to study the heavy-ion reactions. This viewpoint of our study guided us to calculate the estimated value for unobserved fission for the same CN $^{196}$Pt$^*$, at $E_{\mathrm{c.m.}} = 167.2$ MeV, where experimental data are only available for $\sigma_{\mathrm{ER}}$ and $\sigma_{ff}$ is missing. Note, the $\Delta R$ or reaction time is the only parameter of the DCM.

Figure 3 shows the calculated mass fragmentation potential $V(A_2)$ for the best fitted $\Delta R$ values for both ER and ff cross sections at $E_{\mathrm{c.m.}} = 195.2$ MeV ($T = 1.9944$ MeV) for $\ell_{\max} = 158\hbar$ and $\ell = 0$. $\sigma_{\mathrm{ER}}^{\mathrm{Cal.}}$ is fitted ($\equiv \sigma_{\mathrm{ER}}^{\mathrm{Expt.}}$) for $^{196}$Pt$^*$ in both cases ($\Phi_c = 0^\circ$ and $\Phi_c \neq 0^\circ$). The $\ell_{\max}$ value is fixed via Fig. 4, where the calculated $P_0$ is plotted as a function of $\ell$ for the illustrative ER channels. For $\ell_{\max}$, the corresponding ER cross sections go to zero, i.e., the contribution of $P_0$ becomes negligible ($<10^{-10}$). We notice in Fig. 4 that the $1n$ channel has the largest preformation probability as compared to the other three LP channels ($2n$, $3n$, $4n$). Compared to the case of $\Phi_c = 0^\circ$ in Ref. [4], we find that $\ell_{\max}$ increases in going from $\Phi_c = 0^\circ$ to $\Phi_c \neq 0^\circ$, i.e., from $122\hbar$ to $158\hbar$ at $E_{\mathrm{c.m.}} = 195.2$ MeV, and the fragmentation potential $V(A_2)$ of certain fragments (Fig. 3 ) changes due to the nonzero $\Phi_c$ value.

Figure 5 shows the preformation probability $P_0$ as an function of fragment mass number $A_2$. In the DCM $P_0$ is a statistical quantity which gives the structural information of a compound nucleus; according to this factor $^{196}$Pt$^*$ shows the asymmetrical distribution of fission fragments. This factor explains the probable structural aspects of a compound nucleus. In this figure, one can clearly check that at $\ell = 0$ light particles or ERs and at $\ell = 158\hbar$ heavy mass fragments and the fission fragments marked as $A_2 = 51$–$73$ (22 decay fragments from the ff region) are the most probable decay channels.

Next, Fig. 6, shows that three different types of configurations result in different percentages of the compound nucleus

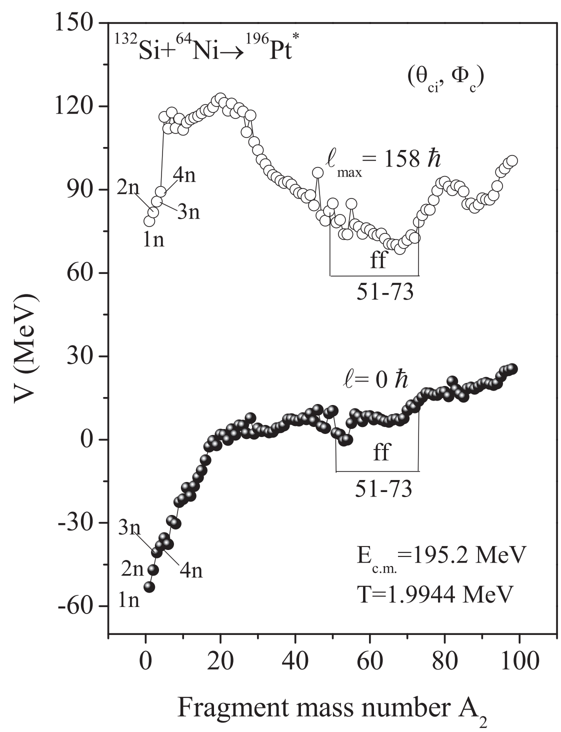


FIG. 3. Mass fragmentation potential minimized in the charge-asymmetry coordinate $\eta_Z$ for the decay of $^{196}$Pt$^*$ formed in the $^{132}$Si + $^{64}$Ni reaction at $E_{\mathrm{c.m.}} = 195.2$ MeV and at $\ell = 0$ and $\ell = 158\hbar$.

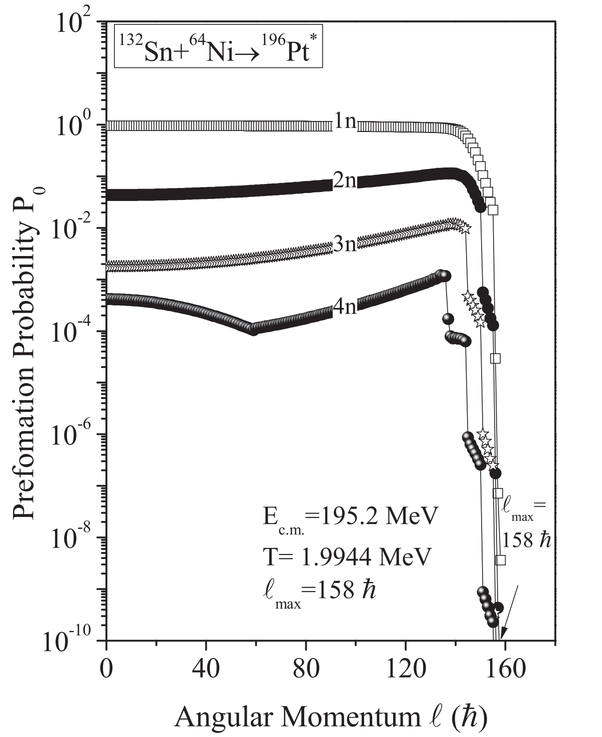


FIG. 4. Preformation probability $P_0$ as a function of angular momentum $\ell$ for ER decays of $^{196}$Pt$^*$ formed in the $^{132}$Sn + $^{64}$Ni reaction at $E_{c.m.}$ = 195.2 MeV. $P_0 \approx 10^{-10}$ for $\ell_{max} = 158\hbar$.

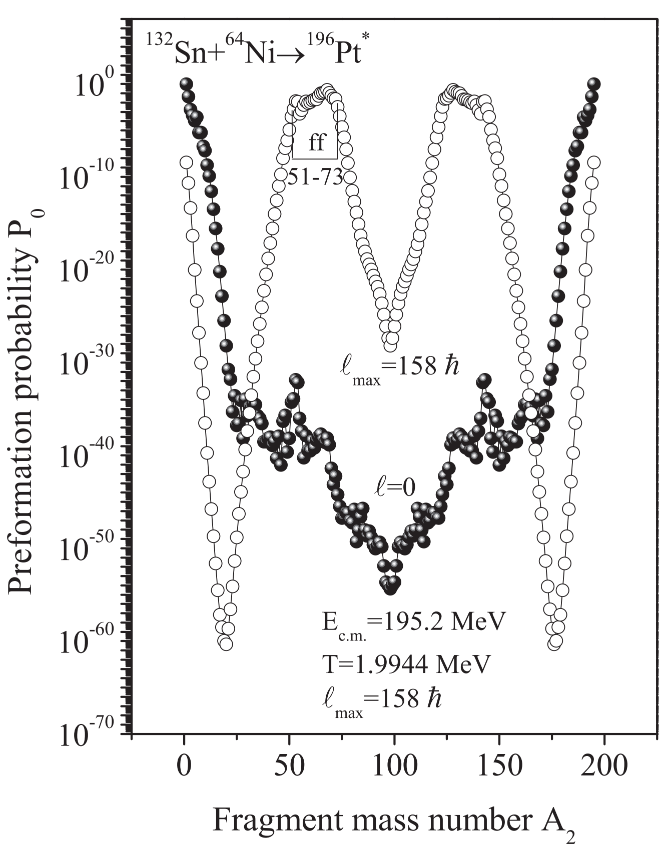


FIG. 5. Preformation probability $P_0$ as a function of fragment mass number for the decay of $^{196}$Pt$^*$ formed in the $^{132}$Si + $^{64}$Ni reaction at $E_{c.m.}$ = 195.2 MeV and at $\ell = 0$ and $\ell = 158\hbar$ values.

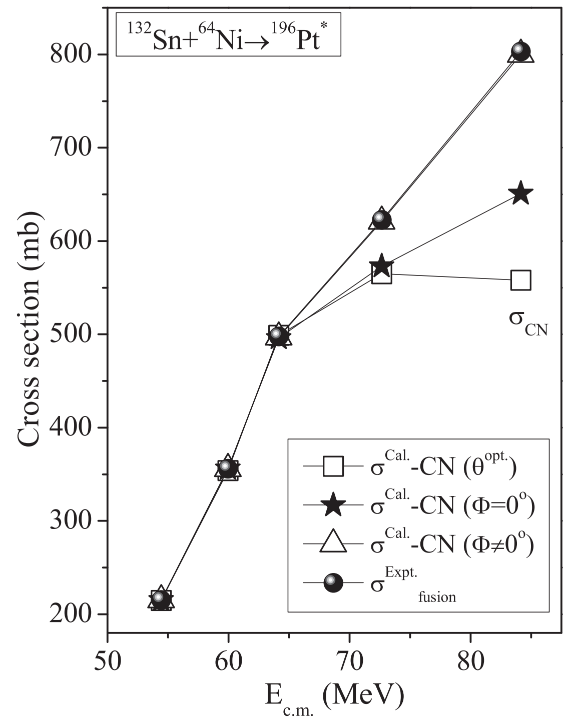


FIG. 6. The DCM-calculated CN cross section, with all three configurations. The experimental data taken from [4] for $\sigma^{\rm Expt.}_{\rm fusion}$ are also shown in the plot.

contributions. The coplanar configuration with only $\theta^{\rm opt.}$ and $\beta_{2i}$ alone shows the largest contribution of nCN at higher energies, then this percentage decreases after the inclusion of $\beta_2$–$\beta_4$, but finally the gap between experimental data and the DCM-calculated cross section gets filled only after the inclusion of noncoplanar degrees of freedom along with the higher multipole deformations ($\beta_2$–$\beta_4$).

Table II presents the DCM-calculated compound nucleus formation probability $P_{\rm CN}$, which shows pure compound nucleus at all energies for the $\Phi_c \neq 0^\circ$ case and for $\Phi_c = 0^\circ$ the $P_{\rm CN} < 1$ at two higher energies.

Figure 7 depicts the possibility for the prediction of the cross section of unobserved decay fragments. This figure shows the best fitted cross-section values of the fission region and evaporation residues. Panel (a) shows that the $\sigma_{ff}$ is exactly matched with the experimental data, whereas in (b) at $E_{c.m.}$ = 167.2 MeV we have only $\sigma_{\rm ER}$, and we have calculated the approximate value of unobserved $\sigma_{ff}$. Our calculations

TABLE II. The comparison of the $\Phi_c \neq 0^\circ$ case with $\Phi_c = 0^\circ$ of DCM-calculated CN formation probability $P_{\rm CN}$ [30] for $^{196}$Pt$^*$.

| $E_{c.m.}$(MeV) | $\Phi_c = 0^\circ$ $P_{\rm CN}$ | $\Phi_c \neq 0^\circ$ $P_{\rm CN}$ |
|---|---|---|
| 195.20 | 0.914 | 1 |
| 183.78 | 0.811 | 1 |
| 175.20 | 1 | 1 |
| 171.00 | 1 | 1 |
| 167.20 | 1 | 1 |
| 165.50 | 1 | 1 |

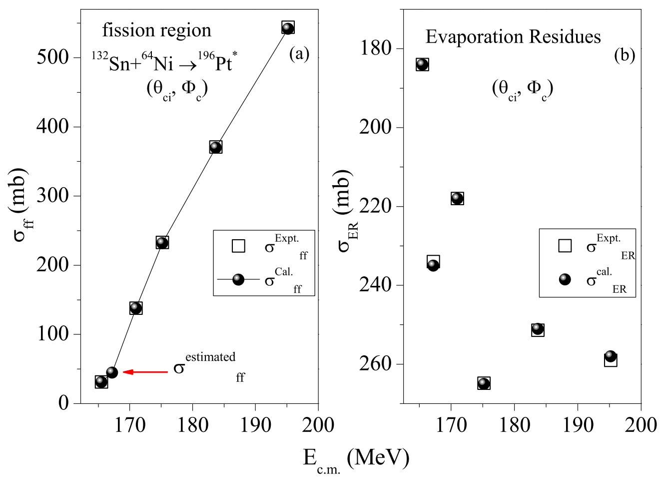


FIG. 7. The DCM-calculated (a) $\sigma_{ff}^{\mathrm{Cal.}}$ and (b) $\sigma_{\mathrm{ER}}^{\mathrm{Cal.}}$, for the $^{132}\mathrm{Sn} + {}^{64}\mathrm{Ni} \rightarrow {}^{196}\mathrm{Pt}^*$ reaction, using the $\Phi_c \neq 0^\circ$ case with $\theta_{ci}$ and higher multipole deformations $\beta_2$–$\beta_4$, plotted as a function of $E_{\mathrm{c.m.}}$, compared with experimental data. In panel (a) we show the DCM-estimated cross section at $E_{\mathrm{c.m.}} = 167.2$ MeV. In panel (b) $\sigma_{\mathrm{ER}}^{\mathrm{Cal.}}$ exactly fitted with experimental data.

provide a good result about unobserved channels, i.e., the estimated number is very close to the measured data and lies on the same curve of other observed channels. In this work we showed that the calculated value of $\Delta R$ for unobserved decay channels (in the fission region) is the well founded number which we have calculated simultaneously along with the valid $\Delta R$ of $\sigma_{\mathrm{ER}}$.

Finally, we have estimated the not-yet-observed ff cross section in the chosen reaction at a particular energy where only $\sigma_{\mathrm{ER}}$ is given, which strongly supports the possibility to find the neck-length parameter to calculate the cross section for the unobserved decay channels. After using the set of parameters ($\theta_{ci}$, $\beta_2$–$\beta4$, and $\Phi_c \neq 0^\circ$) within the DCM, we look forward to experimental validation of predicted cross sections.

## IV. SUMMARY AND CONCLUSIONS

In conclusion, in this paper we have extended the earlier work of Ref. [4] on the decay of $^{196}\mathrm{Pt}^*$ formed in the $^{132}\mathrm{Sn} + {}^{64}\mathrm{Ni}$ reaction at five energies, using the proximity nuclear interaction potential of Blocki *et al.* for coplanar ($\Phi_c = 0^\circ$) and noncoplanar ($\Phi_c \neq 0^\circ$) nuclear configurations. The objective was to see the effect of noncoplanar degrees of freedom on the large noncompound nucleus (nCN) component in the calculated $\sigma_{ff}$ for both configurations, i.e., coplanar ($\Phi_c = 0^\circ$) and noncoplanar ($\Phi_c \neq 0^\circ$), especially at two higher energies. Our calculations are performed with deformation effects included up to hexadecapole with compact orientations of the hot fusion process. The only parameter of the model is the neck-length parameter $\Delta R$, which varies smoothly with the CN excitation energy or temperature of the system, and whose values stay within the nuclear proximity limits of ≈2 fm. Another important result is the estimation of the cross section, which seems to follow the trend of measured data. Most of the calculations are carried out using the dynamical cluster-decay model in reference to experimental data, but we have predicted cross sections for a certain nucleus, as we have done in this work at $E_{\mathrm{c.m.}} = 167.2$ MeV, which could be verified via further experiments. It is concluded that the higher order deformations and noncoplanar degrees of freedom are important tools to address the adequate dynamical evolution of nuclear reactions.

## ACKNOWLEDGMENTS

This work was supported by the department of Physics, Panjab University, Chandigarh, HPCC facility. P.O.H. acknowledges financial support from “Direccion General de Asuntos del Personal Academico UNAM”, PAPIIT-DGAPA (IN100421). We would also like to show our gratitude to (late) Prof. Emeritus Dr. R. K. Gupta for sharing their pearls of wisdom with us.

[1] R. K. Gupta, S. K. Arun, R. Kumar, and Niyti, Int. Rev. Phys. (IREPHY) **2**, 369 (2008).
[2] R. K. Gupta, in *Clusters in Nuclei*, edited by C. Beck, Lecture Notes in Physics 818 (Springer-Verlag, Berlin, 2010), Vol. I, pp. 223-265, and references therein.
[3] J. F. Liang, D. Shapira, J. R. Beene, C. J. Gross, R. L. Varner, A. Galindo-Uribarri, J. Gomez del Campo, P. A. Hausladen, P. E. Mueller, D. W. Stracener, H. Amro, J. J. Kolata, J. D. Bierman, A. L. Caraley, K. L. Jones, Y. Larochelle, W. Loveland, and D. Peterson, Phys. Rev. C **75**, 054607 (2007).
[4] M. K. Sharma, S. Kanwar, G. Sawhney, R. K. Gupta, and W. Greiner, J. Phys. G: Nucl. Part. Phys. **38**, 055104 (2011).
[5] S. Chopra, Hemdeep, P. Kaushal, and R. K. Gupta, Phys. Rev. C **98**, 041603(R) (2018).
[6] M. Manhas and R. K. Gupta, Phys. Rev. C **72**, 024606 (2005).
[7] J. Maruhn and W. Greiner, Phys. Rev. Lett. **32**, 548 (1974).
[8] R. K. Gupta, W. Scheid, and W. Greiner, Phys. Rev. Lett. **35**, 353 (1975).
[9] R. K. Gupta, M. Balasubramaniam, C. Mazzocchi, M. La Commara, and W. Scheid, Phys. Rev. C **65**, 024601 (2002).
[10] R. K. Gupta, R. Kumar, N. K. Dhiman, M. Balasubramaniam, W. Scheid, and C. Beck, Phys. Rev. C **68**, 014610 (2003).
[11] M. Balasubramaniam, R. Kumar, R. K. Gupta, C. Beck, and W. Scheid, J. Phys. G: Nucl. Part. Phys. **29**, 2703 (2003).
[12] G. Royer and J. Mignen, J. Phys. G: Nucl. Part. Phys. **18**, 1781 (1992).
[13] H. S. Khosla, S. S. Malik, and R. K. Gupta, Nucl. Phys. A **513**, 115 (1990).
[14] S. Kumar and R. K. Gupta, Phys. Rev. C **55**, 218 (1997).
[15] R. K. Gupta, S. Kumar, and W. Scheid, Int. J. Mod. Phys. E **6**, 259 (1997).
[16] T. Matsuse, C. Beck, R. Nouicer, and D. Mahboub, Phys. Rev. C **55**, 1380 (1997).
[17] S. J. Sanders, Phys. Rev. C **44**, 2676 (1991).

[18] S. J. Sanders, D. G. Kovar, B. B. Back, C. Beck, D. J. Henderson, R. V. F. Janssens, T. F. Wang, and B. D. Wilkins, Phys. Rev. C **40**, 2091 (1989).
[19] W. Myers and W. J. Swiatecki, Nucl. Phys. **81**, 1 (1966).
[20] A. S. Jensen and J. Damgaard, Nucl. Phys. A **203**, 578 (1973).
[21] N. J. Davidson, S. S. Hsiao, J. Markram, H. G. Miller, and Y. Tzeng, Nucl. Phys. A **570**, 61c (1994).
[22] B. B. Singh, M. K. Sharma, and R. K. Gupta, Phys. Rev. C **77**, 054613 (2008).
[23] G. Audi, A. H. Wapstra, and C. Thiboult, Nucl. Phys. A **729**, 337 (2003).
[24] H. Kröger and W. Scheid, J. Phys. G **6**, L85 (1980).
[25] R. K. Gupta, N. Singh, and M. Manhas, Phys. Rev. C **70**, 034608 (2004).
[26] R. K. Gupta, M. Balasubramaniam, R. Kumar, N. Singh, N. Manhas, and W. Greiner, J. Phys. G: Nucl. Part. Phys. **31**, 631 (2005).
[27] R. K. Gupta, M. Manhas, and W. Greiner, Phys. Rev. C **73**, 054307 (2006).
[28] R. K. Gupta, in *Proceedings of the 5th International Conference n Nuclear Reaction Mechanisms, Varenna, Italy*, edited by Gadioli E (Ricerca Scintifica Educazione Permanente, Rho, Italy, 1988), p. 416.
[29] S. S. Malik and R. K. Gupta, Phys. Rev. C **39**, 1992 (1989).
[30] A. Kaur, S. Chopra, and R. K. Gupta, Phys. Rev. C **90**, 024619 (2014).